The Australian National University
Research School of Physical Sciences

ANU PRL TR 94/1

SHEAR ALFVEN WAVE EXCITATION BY DIRECT ANTENNA COUPLING AND FAST WAVE RESONANT MODE CONVERSION

G. G. Borg

Plasma Research Laboratory

The Australian National University GPO Box 4 Canberra 2601

ANU PRL TR 94/1

SHEAR ALFVEN WAVE EXCITATION BY DIRECT ANTENNA COUPLING AND FAST WAVE RESONANT MODE CONVERSION

G. G. Borg

Plasma Research Laboratory
Research School of Physical Sciences
Australian National University
Canberra ACT 0200
Australia

accepted for publication in
Plasma Physics and Controlled Fusion.

Abstract

Antenna coupling to the shear Alfven wave by both direct excitation and fast wave resonant mode conversion is modelled analytically for a plasma with a one dimensional linear density gradient. We demonstrate the existence of a shear Alfven mode excited directly by the antenna. For localised antennas, this mode propagates as a guided beam along the steady magnetic field lines intersecting the antenna. Shear Alfven wave excitation by resonant mode conversion of a fast wave near the Alfven resonance layer is also demonstrated and we prove that energy is conserved in this process. We compare the efficiency of these two mechanisms of shear Alfven wave excitation and present a simple analytical formula giving the ratio of the coupled powers. Finally, we discuss the interpretation of some experimental results.

1.INTRODUCTION

In the ideal MHD limit, the equation of wave motion in a one dimensionally inhomogeneous magnetised plasma is of second order and has a continuous spectrum of eigenvalues (Hasegawa and Uberoi, 1982). For a fixed parallel wavenumber k_z defined by the antenna, the equation exhibits a resonance at the location which satisfies the Alfven wave dispersion relation, $\omega = k_z v_A$, where v_A is the Alfven speed, $v_A = B_0/(\mu_0\rho)^{1/2}$, B_0 is the steady magnetic field, ρ the plasma mass density and ω the radian frequency. The resonance is referred to as the Alfven or perpendicular ion cyclotron resonance and its location as the Alfven resonance layer (ARL). Qualitatively this solution represents a fast wave which undergoes resonant absorption at the ARL. For low enough damping, the power deposited at the ARL is independent of the damping mechanism (Hasegawa and Chen, 1974, Chen and Hasegawa,1974).

If parallel electron dynamics (PED) is included in the model (finite electron mass, parallel resistivity or finite electron thermal speed), the differential equation of wave motion for fixed k_z becomes fourth order and has four solutions, not all of which need be physically admissible. These solutions physically represent coupled fast-shear wave modes. One of these corresponds physically to the process of resonant absorption where the resonance is resolved by mode conversion of the fast wave to the shear Alfven wave (Swanson, 1989; Hasegawa and Chen, 1976). The shear Alfven wave is a short perpendicular wavelength mode when either electron mass or thermal velocity are included in the model (Ross, Chen and Mahajan, 1982; Vaclavik and Appert, 1991). In a collisionless plasma, the effects of PED depend on the value of β. If $\beta >> m_e/m_i$ the kinetic Alfven wave (KAW) is excited and propagates on the high density side of the ARL. If $\beta << m_e/m_i$ the shear wave is excited whose dispersion is determined by finite electron mass. This latter wave propagates on the low density side of the ARL and has consequently been referred to as the surface quasi-electrostatic wave (SQEW) (Stix T.H., 1980; Vaclavik and Appert, 1991). In the vicinity of the ion cyclotron frequency the SQEW is also referred to as the cold electrostatic ion cyclotron wave CES ICW (Ono, 1993). Provided the shear wave does not interfere with itself after reflection at a boundary, it has been shown that the power transferred from the fast wave to the shear wave is the same as that calculated in the ideal MHD limit for resonant absorption (Hasegawa and Chen, 1975). Shear Alfven wave excitaton by fast wave resonant mode conversion (FWRMC) forms the basis of the Alfven wave heating (AWH) scheme and, in the case of the KAW, has been observed and modelled with satisfactory agreement (Weisen *et. al.*, 1989). Mode conversion to the SQEW has not yet been observed in experiments.

In an infinite homogeneous plasma, the four modes which result when the PED are included in the model are a decoupled fast and shear Alfven wave propagating in each direction. In this limit, both waves are excited directly by the antenna and there is no mode conversion. When excited by a localised antenna with a broad wavenumber spectrum the Fourier wavenumber components of the shear wave superpose to produce a localised beam guided along the lines of the steady magnetic field. Wavefield calculations by various authors for localised antennas in an infinite homogeneous plasma (Schoucri *et. al.*, 1985; Borg, 1987) and group velocity calculations (Borg,1987; Cross,1988a) demonstrate that this property remains substantially true even at finite frequency.

The question naturally arises as to whether this directly excited shear Alfven mode is expected to propagate in an inhomogeneous plasma. If so, how is it coupled to the fast wave and what is the relative efficiency of this process compared with shear wave excitation by FWRMC? The above condition on β can be expressed as $n(m^{-3})\ T(eV) << 10^{21} B^2 (T)$ so that for typical fusion plasma scrape-off layer (SOL) parameters, the SQEW propagates in the plasma periphery and the KAW in the plasma interior. The SQEW is therefore the most likely candidate for direct excitation by an antenna located in the SOL. The process of direct antenna excitation of the SQEW has in fact been noted in some, but not all, numerical antenna-wave coupling simulations for AWH which include the PED (Ross *et. al.*, (1986) and Puri (1987a,1987b)). Here the aim is to optimise the antenna so that direct excitation is minimised, the mode conversion process dominates and power deposition occurs in the plasma interior. Detailed studies of the direct excitation process have not been performed because of the difficulty of differentiating even qualitatively between the directly excited and the mode converted SQEW. In particular, guided Alfven beams formed by Fourier superposition of directly excited shear Alfven waves have not been theoretically predicted for a typical fusion plasma. Recently however Cross (1988b) has demostrated the existence of guided modes which form solutions in the MHD limit.

Experimental evidence for direct excitation is clear. Borg *et. al.* (1985,1987) have confirmed that a small magnetic dipole loop antenna couples to a localised shear Alfven wave beam which propagates for several transits around the circumference of a toroidal plasma along field lines intersecting the antenna before being scattered by limiters and other objects located in the SOL. Experimental results indicate that this wave can propagate in a narrow beam up to the ion cyclotron frequency above which it no longer propagates. The same results have recently been confirmed for an Alfven wave heating antenna (Murphy, 1989). The WKB approximation (Fejer J.A. and Lee K.F., 1967) cannot be applied in these cases because the perpendicular wavefield scale is of the same order as the density gradient scale and the parallel wavelength much longer than the radius of field line curvature. Nonetheless, conditions have been obtained in a laboratory plasma where the WKB approximation applies (Cno, 1979). Moreover, under special conditions, the shear Alfven wave propagation characteristics are quite simple. For example, in a cylindrical plasma with a radially symmetric density gradient, the axisymmetric shear Alfven mode can be excited directly by the antenna and propagates at a local Alfven speed (Cross and Lehane 1968, Cross, 1983). A detailed analysis of this case has been given by Sy (1984).

In this paper we demonstrate the existence of a directly excited shear Alfven wave for the case of non-axisymmetry, $k_y \neq 0$, under conditions where the WKB approximation does not necessarily apply. We address the problem using simple analytical techniques and restrict analysis to the low frequency limit, and a one dimensional linear density variation perpendicular to a constant magnetic field. More ambitious would be to treat the cases of finite frequency and a curved magnetic field. We will also consider for the first time the relative efficiency of the direct excitation and the mode conversion processes. We will present a simple analytical formula for the ratio of the directly excited shear wave to that excited by mode conversion which is valid for modest damping in a slab plasma.

This paper is structured as follows. In section 2 we revise the problem of antenna coupling to Alfven waves in a homogeneous plasma in order to obtain a basic intuition about the shear Alfven wave with finite electron mass. In section 3 we formulate the problem of Alfven wave propagation in an inhomogeneous plasma and discuss energy conservation. In section 4 we consider the antenna-wave coupling problem for an arbitrary inhomogeneity by considering two well known limits for which the exact solutions are known. In section 5 we present some results. Finally in section 6 we conclude with a discussion of the relevance of the results to experimental observations.

2. ANTENNA COUPLING TO ALFVEN WAVES IN A HOMOGENEOUS PLASMA

In this section we consider the limit where the frequency is much lower than the ion cyclotron frequency and finite electron mass is the dominant PED effect so that the SQEW propagates. The case of finite frequency has been treated elsewhere for a homogeneous plasma (Borg, 1987; Shoucri *et. al.* 1985).

We consider a plasma described by the following low frequency dielectric tensor.

$$\varepsilon = \begin{bmatrix} \varepsilon_\perp & 0 & 0 \\ 0 & \varepsilon_\perp & 0 \\ 0 & 0 & \varepsilon_\parallel \end{bmatrix}$$

(1)

where

$$\varepsilon_\perp = c^2/v_A^2 \qquad \varepsilon_\parallel = 1 - \frac{\omega_{pe}^2}{\omega^2} \approx -\varepsilon_\perp/\gamma^2$$

$$\gamma^2 = \frac{\omega(\omega + i\nu_{ei})}{\omega_{ci}\omega_{ce}}$$

$$v_A = \frac{B}{\sqrt{\mu_0\rho}} \qquad \frac{\omega}{\omega_{ci}} << 1 .$$

where ν_{ei} is the election-ion collision frequency and $\omega_{ci,ce}$ respectively the ion, election cyclotron frequency. Here we are also assuming that $\omega >> k_z v_{the}$ where v_{the} is the electron thermal speed. The wave equation is given by,

$$\nabla\times\nabla\times\mathbf{E} = i\omega\mu_0 J_0 + k_0^2\,\varepsilon.\mathbf{E} \tag{2}$$

where k_0^2 is the vacuum wavenumber. For simplicity we consider the following antenna current distribution,

$$J_0 = J_{0z}\left[0, \frac{-k_z}{k_y}, 1\right]\delta(x - b)\,\exp i\left\{k_z z + k_y y - \omega t\right\} \tag{3}$$

where k_z is the wavevector along the steady magnetic field and k_y in the y - direction. The situation is depicted in Fig. 1a. The sheet current automatically satisfies charge conservation since $J_{0y} = -k_z J_{0z}/k_y$ has been assumed. It is a straight forward matter to solve for the wavefields of the fast and slow wave (Borg, 1987). For $\Lambda^2 >> k_A^2$ where $\Lambda^2 = k_y^2 + k_z^2$, the results obtained for the E_y components of the fast wave and SQEW are respectively,

$$E_y = \frac{-i\omega\mu_0 k_z \Lambda J_{0z} e^{-\Lambda x}}{2k_y\left[k_z^2 - k_A^2\right]} \tag{4a}$$

$$E_y = \frac{-\omega\mu_0 k_z k_y J_{0z} e^{-ik_s x}}{2k_s\left[k_z^2 - k_A^2\right]} \tag{4b}$$

E_y is related to E_z for the SQEW by,

$$\left[k^2 - k_A^2\right] E_y = i\omega\mu_0 J_{0y} + k_y k_z\left(1 + \frac{1}{\gamma^2}\right) E_z \qquad (4c)$$

where $k_A = \omega/v_A$ is the Alfven wave number and $k = (\Lambda^2 + k_x^2)^{1/2}$ is the total wavenumber. In equation (4b), the slow wavevector in the x-direction is given by,

$$k_S = \sqrt{\frac{k_z^2 - k_A^2}{\gamma^2} - k_y^2} \qquad (4d)$$

Notice that the fast wave is an evanescent vacuum field which cannot couple energy to a homogeneous plasma. This is very different to the case of an inhomogeneous plasma as we shall see. The SQEW is backward propagating in the x-direction and is launched solely by the z-directed elements of the antenna (Borg, 1987). Unlike the fast wave it also propagates down to very low density where $\epsilon_\parallel \approx 0$. The power per unit area radiated by the antenna into a SQEW propagating in one direction is given by

$$P_f = \frac{k_S(k_z^2 - k_A^2)\, k_A^2}{2\mu_0\omega\, k_z^2\, k_y^2} |E_y|^2 \qquad (5)$$

Equation (5) can be shown to be in agreement with Stix's formula (Stix, 1992b) for the energy transported by a plasma wave when the dielectric tensor of equation (1) is applied. The energy of the SQEW is transported by coherent particle motions. It is easy to show that in this low frequency limit, the SQEW has no magnetic field component b_z along the steady field and that in the limit $k_z >> k_A$, has no magnetic field at all. In this low density limit the SQEW therefore becomes electrostatic. For $k_z < k_A$ the SQEW is evanescent. The SQEW has some other interesting properties. The ratio of the density perturbation to average density is given by (Donnelly and Cramer, 1986),

$$i\omega\frac{\bar{n}}{n} = \frac{dn/dx}{n}\frac{E_y}{B} + \frac{i\omega b_z}{B} + \frac{i\omega\epsilon_0\epsilon_\parallel}{ne}\frac{\partial E_z}{\partial z} \qquad (6)$$

where n is the equilibrium density. In a homogeneous plasma and for $b_z = 0$ only the third term remains. Taking $P_f = 10\ kW/m^2$ in equation (5), $k_z >> k_A$ (in SI units) frequency = 1 MHz, B = 1 T in hydrogen and $n = 10^{18}\ m^{-3}$ then,

$$\frac{\bar{n}}{n} \approx 0.20 k_z^{3/2}$$

The SQEW can therefore have a very high density fluctuation level which increases with the imposed k_z.

As k_A approaches zero the dispersion relation (4d) reads $k_z/k_\perp = \gamma$ where $k_\perp{}^2 = k_S{}^2 + k_y{}^2$ and, as for the lower hybrid wave, the SQEW excited by a localised antenna propagates along the magnetic field with a resonance cone of angle $\theta = \tan^{-1}(\gamma)$ (Ono, 1979). Similarly one may show using (4d) that the group velocity of the SQEW is directed mainly along the magnetic field of a homogeneous plasma. Either way, we obtain the well known result that a SQEW wavepacket is guided by the magnetic field.

It is of interest to know whether these properties remain valid for an antenna located in an inhomogeneous plasma for which the imposed k_y and k_z are of the order of the spatial scale of the density and magnetic field. We aim to justify the assertion that direct excitation of the SQEW by an antenna can be successfully modelled by the homogeneous plasma limit for plasma conditions typical of AWH in toroidal devices.

3. ALFVEN WAVE PROPAGATION IN AN INHOMOGENEOUS PLASMA

We again consider wave propagation in the low frequency limit. In an inhomogeneous plasma, difficulties arise at finite frequency due to the appearance of a cut-off, resonance, cut-off triplet in the MHD model fast wave dispersion (Stix, 1992a). At low frequency, these critical frequencies merge together and complicate the asymptotic analysis of the fourth order model including the PED. In what follows, we will avoid this problem by seeking full wave solutions in closed form to supplement the asymptotic formulae.

3a THE DIFFERENTIAL EQUATION OF WAVE MOTION

We consider the problem depicted in Fig 1b with linear density profile and a homogeneous plasma SOL. We let the Alfven wavenumber be specified by,

$$k_A^2 = k_a^2\left(1 + x/\Delta\right) \tag{7}$$

where k_a is the value of the Alfven wavenumber in the homogeneous plasma SOL region for $x < 0$. For $x > 0$ the following differential equations for E_y and E_z are obtained from the wave equation (2) after eliminating E_x,

$$k_z^2\left[\frac{d^2E_y}{dx^2} - \left(\Lambda^2 - k_A^2\right)E_y\right] = k_yk_z\left[\frac{d^2E_z}{dx^2} - \left(\Lambda^2 + \frac{k_A^2}{\gamma^2}\right)E_z\right] \tag{8a}$$

$$\frac{d}{dx}\left(\frac{k_z^2 - k_A^2}{\Lambda^2 - k_A^2}\right)\frac{dE_y}{dx} - \left(k_z^2 - k_A^2\right)E_y = k_yk_z\left\{\frac{d}{dx}\left[\frac{dE_z/dx}{\Lambda^2 - k_A^2}\right] - E_z\right\} \tag{8b}$$

If we assume that $\Lambda^2 >> k_A^2$ for all x such that $k_A^2(x) < k_z^2$ then equations (8) can be rewritten to lowest order in k_a^2/Λ^2 as,

$$k_z^2\left[\frac{d^2E_y}{dx^2} - \Lambda^2E_y\right] = k_yk_z\left[\frac{d^2E_z}{dx^2} - \left(\Lambda^2 + \frac{k_A^2}{\gamma^2}\right)E_z\right] \tag{9a}$$

$$\frac{d}{dx}\left[k_z^2 - k_A^2\right]\frac{dE_y}{dx} - \Lambda^2\left(k_z^2 - k_A^2\right)E_y = k_yk_z\left\{\frac{d^2E_z}{dx^2} - \Lambda^2E_z\right\} \tag{9b}$$

This is feasible for the density profile of Fig. 1b because the SQEW is evanescent at densities for which $k_A^2(x) > k_z^2$.

3b ENERGY CONSERVATION

The x-component of Poynting flux is defined by,

$$P_x = \frac{1}{2\mu_0}\mathrm{Re}\left\{E_y^*b_z - E_z^*b_y\right\} \tag{10}$$

After substituting for b_z and b_y from Faraday's equation and for E_x from the x-component of the wave equation (2) one obtains,

$$P_x = \frac{1}{2\omega\mu_0} \mathrm{Im}\left\{\left[k_z^2 - k_A^2\right] E_y^* \frac{dE_y}{dx} + \left[k_y^2 - k_A^2\right] E_z^* \frac{dE_z}{dx} - k_y k_z \left[E_z^* \frac{dE_y}{dx} + E_y^* \frac{dE_z}{dx}\right]\right\}$$

(11)

It may be shown that if (9a) is multiplied by $E_z^* k_y/k_z$ and is subtracted from equation (9b) multiplied by E_y^* then the following expression is obtained after integration,

$$\Delta T = \frac{1}{2\omega\mu_0} \mathrm{Im} \int_{x_1}^{x_2} dx \left\{\frac{k_y^2 k_A^2 |E_z^2|}{\gamma^2}\right\} \qquad (12)$$

where

$$T = \frac{1}{2\omega\mu_0} \mathrm{Im}\left\{\left[k_z^2 - k_A^2\right] E_y^* \frac{dE_y}{dx} + k_y^2 E_z^* \frac{dE_z}{dx} - k_y k_z \left[E_z^* \frac{dE_y}{dx} + E_y^* \frac{dE_z}{dx}\right]\right\}$$

(13)

and x_1 and x_2 are arbitrary x-values at which T is evaluated and $\Delta T = T(x_2) - T(x_1)$. In the absence of damping $\Delta T = 0$. Since $T = P_x$ except for a term proportional to k_A^2 we conclude from equations (12) and (13) that equations (9a) and (9b) conserve the Poynting flux to lowest order in k_a^2/k_y^2.

Conservation of energy in the sense of equations (12) and (13) has to be satisfied by all solutions obtained to equations (9).

4 SOLUTION OF THE WAVE EQUATION

Equations (9) can be combined to yield the following fourth order differential equation,

$$\frac{d^4E_y}{dX^4} + \lambda^2\left\{\frac{d}{dX}\left(X\frac{dE_y}{dX}\right) - \delta^2\left(X + \frac{\delta^2}{\lambda^2}\right)E_y\right\} = \left[\frac{d^2}{dX^2} - \delta^2\right]\frac{dE_y/dX}{(\alpha + 1 - X)}$$

(14)

where $\delta = \Delta\Lambda$, $\lambda = k_a\Delta/\gamma$ and

$$X = \alpha - x/\Delta$$

$$\alpha = \left[k_z^2 - k_a^2 - 2\gamma^2\Lambda^2\right]/k_a^2$$

In X-coordinates the ARL is located at $X = 0$ and the low density side of the ARL is located at $X > 0$ where the SQEW propagates. Many similar fourth order differential equations have been obtained for various wave heating scenarii involving mode conversion (Stix, 1965; Bellan and Porkolab, 1974; Ngan and Swanson, 1977; Perkins, 1977; Faulconer, 1980; Swanson, 1989; Stix, 1992)

The solution to equation (14) can be written down in closed form by employing the method of the generalised Laplace transform (Swanson 1989). Before doing so however we approximate the right hand side of equation (14) by replacing $\alpha+1-X$ in the denominator by a constant D. We will soon show that this term does not contribute in lowest order to the asymptotic expansion of E_y for large X. Consider the following representation of E_y,

$$E_y(X) = \int_C dt\, \tilde{E}_y(t)\, e^{tX} \tag{15}$$

where C is an arbitrary contour in the complex t-plane. We apply the differential operator of equation (14) to equation (15) and integrate the terms containing X once by parts. We choose the contour C so that the integrand vanishes at the endpoints where $|t| \to \infty$. It is easy to show that this procedure leads to the following first order differential equation for the Laplace transform,

$$\frac{d\tilde{E}_y}{dt} - \frac{1}{\lambda^2}\left\{t^2 + \delta^2 - \frac{\lambda^2 t}{t^2 - \delta^2} - \frac{t}{D}\right\}\tilde{E}_y = 0$$

This may be integrated directly and substituted back into equation (15) to yield,

$$E_y(X) = \int_C dt\, \frac{\exp\{\phi(t)\}}{\sqrt{t^2 - \delta^2}} \tag{16}$$

where

$$\phi(t) = t\left(X + \frac{\delta^2}{\lambda^2}\right) + \frac{t^3}{3\lambda^2} - \frac{t^2}{2D\lambda^2}$$

In equation (16) we make the substitution $t = -\lambda|X + \delta^2/\lambda^2|^{1/2}p$ to obtain the following integral representation of $E_y(X)$,

$$E_y(X) = \int_C dp\, \frac{\exp\{Lw(p)\}}{\sqrt{p^2 - p_B^2}} \tag{17}$$

$$w(p) = -\left\{p\,\mathrm{sgn}\left(X + \frac{\delta^2}{\lambda^2}\right) + \frac{p^3}{3} + \frac{p^2}{2D\lambda|X + \delta^2/\lambda^2|^{1/2}}\right\}$$

$$L = \lambda\left|X + \frac{\delta^2}{\lambda^2}\right|^{3/2} \quad \text{and} \quad p_B = \frac{\delta}{\lambda\left|X + \frac{\delta^2}{\lambda^2}\right|^{1/2}}$$

Equation (17) is amenable to solution by asymptotic techniques. For large values of L the third term in the expression for w(p) can be neglected justifying our previous assumption of letting D be constant. We shall soon see however that energy conservation does depend on this equilibrium gradient term. For the following analysis we therefore approximate,

$$w(p) \approx -\left\{p\,\mathrm{sgn}\left(X + \frac{\delta^2}{\lambda^2}\right) + \frac{p^3}{3}\right\} \tag{18}$$

In order to solve equation (14) we need to invert (17) for different contours in the complex plane until all physically meaningful solutions are obtained. In practice, equation (14) has four linearly independent solutions. We shall find that for the problem depicted in Fig. 1b there are two solutions of physical significance.

4a FAST WAVE RESONANT MODE CONVERSION TO THE SHEAR ALFVEN WAVE

In order to obtain the usual solution to equation (14) describing FWRMC we first consider the well known MHD solution. When $\lambda \to \infty$, finite electron mass effects are eliminated from the physics, the SQEW no longer propagates and equation (14) simplifies to the following second order differential equation,

$$\frac{d}{dX}\left(X\frac{dE_y}{dX}\right) - \delta^2 X E_y = 0 \tag{19}$$

Equation (19) is recognised as the usual modified Bessel equation describing the MHD limit (Hasegawa and Chen, 1974, Chen and Hasegawa,1974). This equation has the solution,

$$E_y = E_{y0}\, K_0[-\delta X]$$

where K_0 is the McDonald function which satisfies $E_y \to 0$ as $X \to -\infty$ and has to be analytically continued for $X > 0$ to give,

$$E_y = E_{y0}\,[K_0(\delta X) - i\pi\, I_0(\delta X)]$$

This solution represents the fast wave of ideal MHD. As previously mentioned, the solution has a singularity at the ARL, $X = 0$. It may be shown that the power coupled per unit area by the fast wave to the ARL is given by (Hasegawa and Chen, 1974, Chen and Hasegawa,1974),

$$P_f = \frac{\pi\, k_a^2\, |E_{y0}|^2}{2\,\mu_0\,\omega\,\Delta\,\Lambda^2} \tag{20}$$

To the best of the author's knowledge, the method of the generalised Laplace transform has not been applied to obtain the solution to equation (14) describing FWRMC. Moreover, it has never been shown analytically that the KAW (or the SQEW) actually tranports this energy away from the ARL. Given the vast difference in the physics of equations (14) and (19), it would provide an important test of the present calculation to show that the energy transported by the mode converted SQEW according to equation (5) is indeed given by equation (20). This is the task to which we now turn.

We first obtain the solution to equation (19) by the Laplace transform technique since this will enable us to infer directly the solution to equation (17). The Laplace transform has the following simplified form of w(p),

$$w(p) \approx -p\,\mathrm{sgn}(X) \tag{21}$$

We make the substitution $p = ip_B\sinh(u)$ in equation (17) using (21) and define,

$$E_y(X) = K_0(-\delta X) = \frac{1}{2}\int_C du \exp\{-i\ \delta X \sinh[u]\} \tag{22}$$

Expression (22) is a well known integral representation of the McDonald function where C denotes the contour depicted in Fig. 2a of the complex u-plane (Davies, 1978)

After making the same substitution in equation (17) using (18) we obtain the following expression for E_y,

$$E_y^M(X) = \int_C du \exp\{ Lp_B\ V(u)\}$$

$$V(u) = -i\left[\mathrm{sgn}(X)\sinh(u) - p_B^2\sinh^3[u]/3\right] \tag{23}$$

where $|X| >> \delta^2/\lambda^2$ has been assumed. The contour C is similar to that of Fig. 2a and is depicted in Fig. 2b for the case where $X > 0$ and Fig. 2c for $X < 0$. The contour has to be chosen as usual so that the integrand of (23) approaches zero as $|u| \to \infty$. The hatched regions indicate where this condition is satisfied.

An aymptotic solution to integral (23) can now be obtained by the method of steepest descents (Bleistein and Handelsmann, 1975a). For ease of visualisation, the level curves of the real part of V(u) are shown plotted in Fig. 3. This plot indicates where the exponential in (23) is important and provides visual confirmation of the choice of contour. The saddle points of the real part of V(u) are the points in the complex u-plane where V(u) is stationary. These are given by $\sinh^2(u) = 1/p_B$ and $\cosh(u) = 0$ and are marked by crosses in Figs. 2 and 3. The contour C has been deformed so that it passes through the saddle points of the real part of V(u) along the directions of steepest descent.

For $X > 0$, the directions of steepest descent in Fig. 2b are given by $\arg(u) = \pi/4$ for $\sinh(u) = 1/p_B$ in each case and $\arg(u) = \pi/2$ for $\cosh(u) = 0$. For $X > 0$, the first term of the asymptotic expansion valid to largest order in $Lp_B = \delta|X|$ is then,

$$E_y^M(X) \approx \sqrt{\frac{4\pi}{\lambda|X|^{3/2}}} \exp i\left\{-\frac{2}{3}\lambda|X|^{3/2} + \frac{\pi}{4}\right\} + 2K_0[-\delta X] \tag{24a}$$

For $X < 0$, the directions of steepest descent are given by $\arg(u) = \pm\pi/2$ for $\sinh(u) = 1/p_B$ and $\arg(u) = 0$ and π for $\cosh(u) = 0$. The solution is given by,

$$E_y^M(X) \approx \sqrt{\frac{\pi}{\lambda|X|^{3/2}}} \exp\left\{-\frac{2}{3}\lambda|X|^{3/2} - \frac{\pi i}{2}\right\} + 2K_0[-\delta X] \tag{24b}$$

Here we have replaced the asymptotic part for the fast wave due to the saddle points of $\cosh(u) = 0$ by the McDonald function, but it must be borne in mind that equation (23) is not valid near X = 0. Equation (24) like equation (17) is in particular not singular at X = 0 as in the MHD case. For X > 0 there is an additional term with the SQEW wavenumber which propagates on the low density side of the ARL as expected. This wave is backward propagating since it propagates toward X = 0 when its energy propagates toward X = +∞. For X < 0, the solution consists of an evanescent SQEW and the fast wave represented by the McDonald function. As in the case of ideal MHD, the fast wave is described by the McDonald function of a negative argument for X > 0 and a positive argument for X < 0. Analytic continuation for X > 0 therefore produces the I_0-Bessel function required to describe a fast wave launched by the antenna. Solution (24) therefore represents the case of SQEW excitation by FWRMC. We now demonstrate that energy is conserved.

Direct substitution of equation (24) into equation (14) proves that it satisfies the differential equation to highest order, λ^4 irrespective of the coefficient of the exponential term in equation (24). Solution (24) also satisfies equation (14) to λ^3 with the above coefficient provided we ignore the equilibrium gradient term on the right hand side of equation (14) as previously assumed. It is also easy to check that if we substitute this coefficient for the SQEW into equation 5, we do not obtain equation 20. If on the other hand, we retain the equilibrium gradient term and use the form of w(p) given in equation (17), then one can only obtain an asymptotic expansion by assuming that $k_z = k_a = k_A$. If in addition $\lambda X^{3/2}$ >> 1 near x = 0 (X = α) then D = 1 and equation (23) becomes,

$$V(u) = -i\left[\mathrm{sgn}(X)\sinh(u) - p_B^2\sinh^3[u]/3 + \frac{ip_B^2\sinh^2[u]}{2\lambda|X|^{1/2}}\right] \tag{25}$$

In this case the asymptotic expansion for X > 0 is given by,

$$E_y^M(X) \approx \sqrt{\frac{4\pi}{\lambda|X|^{3/2}}}\exp\left\{i\left[-\frac{2}{3}\lambda|X|^{3/2} + \frac{\pi}{4}\right] + \frac{X}{2}\right\} - 2K_0[-\delta X] \tag{26}$$

Since $X = (k_z^2 - k_a^2 - 2\gamma^2\Lambda^2)/k_a^2 << 1$ we may write $\exp(X) = 1 + (k_z^2 - k_a^2 - 2\gamma^2\Lambda^2)/k_a^2 = (k_z^2 - 2\gamma^2\Lambda^2)/k_a^2 = k_z^2/k_a^2$. We therefore have $\exp(X/2) = k_z/k_a$. From equation (26) the ratio of SQEW to fast wave amplitude therefore becomes,

$$\frac{E_{y0}(SQEW)}{E_{y0}(fast)} = \sqrt{\frac{\pi\gamma k_z^2}{\Delta\left(k_z^2 - k_a^2\right)^{3/2}}}, \tag{27}$$

and substitution into equation (5) is equal to equation (20) in the limit where $\Lambda = k_y$. In fact it is possible to evaluate the coefficient of the SQEW exponential term in equation (24) assuming D = α+1- X. Substitution of $E_y = \Psi(X)\exp i(-2\lambda|X|^{3/2}/3 + \pi/4)$ directly into equation (14) yields a simple expression for Ψ after setting the coefficient of λ^3 to zero. The amplitude Ψ is only determined to within a multiplying factor by this technique but by comparison with equation (27) we note that,

$$\Psi(X) = \sqrt{\frac{4\pi}{\lambda X^{3/2}}}\,\frac{k_z}{k_A(X)}\,\frac{k_y}{\Lambda} \tag{28}$$

satisfies energy conservation. Equation (28) indicates that the amplitude of the SQEW adjusts itself at each value of X to keep the power flux of equation (5) equal to the value of equation (20). This agrees with the conclusions of Hasegawa and Chen (1975).

This concludes the discussion of SQEW excitation by FWRMC. We have demonstrated the important result that the energy lost by the fast wave is transported away from the ARL by the SQEW. Energy conservation however requires the equilibrium gradient term in equation (14). The FWRMC solution was obtained in analogy with the ideal MHD case of resonant absorption.

4b DIRECT EXCITATION OF THE SHEAR ALFVEN WAVE

A second solution to equation (14) can be obtained directly from equation (17). Firstly however we consider an approximate solution to equation (14) valid in the limit where $Lp_B^3/3 \gg 1$ or $\delta^3 \gg \lambda^2$. Equation (17) now simplifies to the following integral representation,

$$E_y(X) = \frac{1}{ip_B}\int_C dp \ \exp\{Lw(p)\} \tag{29}$$

where w(p) is defined in equation (18). It is easy to show that the corresponding form of equation (14) in this approximation is given by,

$$\left\{\frac{d^2}{dX^2} - \delta^2\right\}\left\{\frac{d^2E_y}{dX^2} + \lambda^2\left(X+\frac{\delta^2}{\lambda^2}\right)E_y\right\} = 0 \tag{30}$$

The first operator in equation (30) describes the fast wave of a homogeneous plasma. There is no resonant absorption in this model because the fast wave solution is not singular nor is there any mode conversion because the fourth order differential equation has separated into two decoupled second order differential equations. The second operator is the differential equation for the Airy function and describes a SQEW which propagates independently of the fast wave. Its solution is given by,

$$E_y = Ai\left\{-\lambda^{2/3}\left(X + \frac{\delta^2}{\lambda^2}\right)\right\} \tag{31}$$

where Ai is the Airy function. The Ai - Airy function is chosen by requiring that the SQEW fields remain bounded as $X \to -\infty$. This expression describes a standing SQEW which originates in the plasma boundary and propagates toward the Alfven resonance layer at X = 0 where it is reflected. It is clear that this solution is a WKB-like approximation for a near homogeneous plasma with the important difference expected from the dispersion relation of equation (4d) that the SQEW undergoes cut-off at the ARL. This follows because for $k_z < k_a$, k_x becomes imaginary. The SQEW must therefore form a standing wave on the low density side of the ARL after being excited directly by the antenna. Solution of equation (30) by Green's functions for the geometry of Fig. 1b confirms this remark. In addition, besides the usual mechanism of SQEW excitation by z-directed current elements, the solution obtained indicates that x-directed ('radial feeders') of the antenna couple to the wave provided the antenna feeds are located in the density gradient.

As in the previous section, solution of equation (30) by the method of the generalised Laplace transform reveals the contour integral required to solve equation (17). A contour integral representation of the Ai-Airy function is shown in Fig. 4a (Bleistein and Handelsmann, 1975b) for the integral of equation (29). For $X > 0$ the contours C_1 and C_2 have to be chosen and for $X < 0$ the contour C_3 has to be chosen in order to generate the Ai-Airy function. The integrands in equations (17) and (29) vanish at $|p| \to \infty$ along these contours in the complex p-plane provided they approach infinity inside the sectors arg(p) $\in [-\pi/6,\pi/6]$, $[\pi/2,5\pi/6]$ or $[7\pi/6,3\pi/2]$. The corresponding level curves are shown in Fig. 5. From Cauchy's theorem, either $C_1 \cup C_2$ or C_3 can be distorted onto the imaginary p axis to obtain the following well known integral representaion (Abramowitz and Stegun, 1970a),

$$\mathrm{Ai}\left\{-\lambda^{2/3}\left(X + \frac{\delta^2}{\lambda^2}\right)\right\} = \frac{\lambda^{1/3}\left|X+\delta^2/\lambda^2\right|^{1/2}}{\pi}\int_0^{\infty} dt\,\cos\left\{L\left[t\,\mathrm{sgn}\left(X + \frac{\delta^2}{\lambda^2}\right) - t^3/3\right]\right\} \tag{32}$$

The analogous contours for equation (17) are shown in Fig. 4b. These contours are the same except for the branch cuts arising from the branch point singularities at $p = \pm p_B$ in equation (17). An integral representation for equation (17) can also be obtained in a similar manner to that of equation (32) by evaluating the integral along the imaginary p-axis,

$$E_y(X) = 2\int_0^{\infty} dp\,\frac{\cos\left\{L\left[p\,\mathrm{sgn}(X) - p^3/3\right]\right\}}{\sqrt{p^2 + p_B^2}} \tag{33}$$

Not surprisingly, E_y in this case is a cross between the McDonald function of a positive argument and the Ai-Airy function of equation (32) (Abramowitz and Stegun, 1970a, 1970b). Once again however there is no singularity at $X = 0$. It is important to note that the McDonald function has a positive argument for both $X > 0$ and $X < 0$.

Unlike the fast wave function in equation (23), the fast wave solution here decreases on both sides of the ARL and is not suitable for representing a fast wave excited by an external antenna. Equation (33) is therefore a second linearly independent solution to equation (14).

In Fig. 4b the saddle points of the integrand of equation (17) are given by $p^2 = -1$ and the asymptotic form of the McDonald function is obtained by evaluating the loop integral around the branch cut. The asymptotic solution for $X > 0$ is given by,

$$E_y^D(X) = -\sqrt{\frac{4\pi}{\lambda|X|^{3/2}}}\,\sin\left\{\frac{2}{3}\lambda|X|^{3/2} + \frac{\pi}{4}\right\} - 2K_0\left[\delta|X|\right] \tag{34a}$$

This solution is very similar to equation (31) and has a similar interpretation. The sine function represents a standing SQEW as mentioned above. The main difference is the additional fast wave term which we have represented by the McDonald function although the solution is again asymptotic and not valid near $X = 0$. This equation should be compared to equation (24a) describing a SQEW excited by FWRMC. From equation (34a) we see that the amplitude of the wave is determined by the boundary conditions satisfied by the SQEW wavefields at the antenna because the McDonald function is exponentially small far from and on either side of the ARL at $X = 0$. This is important because in the presence of reasonable damping we may neglect the effect of the equilibrium gradient term in equation (14) on the amplitude term of the SQEW in equation (34a). In the absence of damping however, the same correction (equation 28) to the amplitude of equation (24a) as a result of the equilibrium gradient term is expected to apply to equation (34a) because equations (24a) and (34a) both satisfy equation (14). As we shall soon see, for the conditions of a typical laboratory plasma, the SQEW term in equation (34a) dominates over the McDonald fast wave function. For $X < 0$ the saddle point is at $p = -1$ and the solution is given by,

$$E_y^D(X) = \sqrt{\frac{\pi}{\lambda|X|^{3/2}}}\exp\left(-\frac{2}{3}\lambda|X|^{3/2} - \frac{\pi i}{2}\right) - 2K_0[\delta|X|]$$

(34b)

Equation (34b) describes an evanescent SQEW for $X < 0$ as expected. We conclude that equations (34) represent a SQEW mode excited directly by the antenna.

5 ANTENNA COUPLING RESULTS

We have obtained two solutions to equation (14). Each solution represents an excited SQEW. Solution (24) which corresponds to the MHD limit case of resonant absorption describes a SQEW excited by FWRMC. Solution (34) corresponding to the WKB or a homogeneous plasma limit describes a SQEW excited directly by the antenna. Far from the ARL this wave propagates independently of the fast wave.

It is relatively straightforward to use the asymptotic solutions (24) and (34) to equation (14) to calculate the total wavefield excited by the antenna of equation (3) for the situation depicted in Fig. 1b. The solutions in the SOL region consist of equations (4a) and (4b) plus two reflected waves from the interface at $x = 0$ each with an unknown constant multiplying factor. There are also two unknown constants multiplying the solutions (24) and (34) for $x > 0$. These four unknown constants are determined by four boundary conditions satisfied by E_y at the $x = 0$ interface. The boundary conditions which are derivable from equation (14) are that E_y and its first three derivatives are continuous across the $x = 0$ interface.

A sample wavefield is shown in Fig. 6 for conditions typical of a medium sized tokamak. This calculation is for $k_a = 1.0$, $k_z = 2.0$, $k_y = 20$ radians per metre, $\Delta = 0.05$ m and for modest damping where $\gamma = (1 + 0.05i) \times 10^{-3}$. The directly excited SQEW can be clearly seen near the antenna to the left and the asymptotic remainder of the mode converted SQEW to the right near the ARL. The equilibrium gradient term has been included in these calculations so that for the case of high damping the total power radiated by the antenna is equal to the sum of the direct SQEW and the mode converted SQEW. In the case of low damping, the SQEW propagating to the left of the antenna carries all the antenna radiated power.

Fig. 7 shows the ratio of the power coupled by the antenna to the SQEW to that of the fast wave for the same conditions of Fig. 6 but as a function of various transverse wavenumbers, k_y. These results are plotted as points. The increase of this ratio with k_y is due to the decrease of the power coupled to the mode converted SQEW with increasing k_y as a result of the fast wave cut-off. The lower mode numbers $k_y < 10$ radians per metre are in fact typical of AWH. This reaffirms the conclusion that low non-zero poloidal mode numbers (especially $m = 1$) are best for FWRMC. For localised antennas, the high k_y

cannot be ignored and if desired can be preferentially excited.

For this case of modest damping where the directly excited SQEW does not interfere with itself after reflection from the ARL and where the mode converted SQEW does not interfere with itself after reflection from the boundary, the above ratio ought to be simply given by that of the direct SQEW power as calculated for a homogeneous plasma from equations (4b) and 5 to the power calculated for the ideal MHD fast wave from equation 20 and the geometry of Fig 1b. For the case of Fig. 1b, the ideal MHD fast wavefield is given by,

$$E_y(x) = \frac{-i\omega\mu_0 k_z \Lambda J_{0z} \exp(-\Lambda b)\, K_0[(x-\alpha\Delta)\Lambda]}{k_y \left[k_z^2 - k_A^2\right] Q} \qquad (35)$$

where,

$$Q = [K_0(\alpha\Delta\Lambda) - K_1(\alpha\Delta\Lambda)] - i\pi\,[I_0(\alpha\Delta\Lambda) + I_1(\alpha\Delta\Lambda)]$$

and $x = -b$ is the location of the antenna in Fig. 1b. The power coupled into the mode converted SQEW is then given by substituting the amplitude of equation 35 into equation 20. The final result is,

$$\frac{P_D}{P_M} = \frac{\Delta k_y^2 \left[k_z^2 - k_A^2\right] |Q|^2 \exp(2b\Lambda)}{2\pi\, k_S\, k_z^2} \qquad (36)$$

where P_D and P_M are the powers coupled respectively to the directly excited SQEW and the SQEW after mode conversion. This ratio has been plotted over the points in Fig. 7. We conclude that the simple analytical result of equation 36 provides a good approximation in the modest damping limit.

Although the model presented in Fig. 1b (or the case of a continuously linear variation of the density at the antenna) is probably the most realistic SOL model for a one dimensional plasma, it is important to examine the nature of the wavefields excited by the same sheet antenna for other commonly used models of the SOL. We now consider the cases where the SOL is modelled by a low density plasma and by a vacuum region. We wish to conclude whether the antenna excitation efficiencies of the directly excited and the mode converted SQEWs predicted by these models are in agreement. The boundary conditions assumed are that E_y, E_z, b_y, b_z are continuous across a plasma-plasma or a plasma-vacuum interface for the case of finite electron mass. We also assume for the moment that the damping is sufficiently large that the SQEW is damped between the boundary and the ARL.

For the case of an infinite homogeneous plasma (equations 4a) and $\Lambda^2 >> k_a^2$, the fast wave is a cut-off mode. For a low density plasma or vacuum region however, it is easily verified that the fast wave can propagate with $k_x^2 = -\Lambda^2$. This mode is referred to as the surface wave (SW) and is discussed in detail by Cross (1988a) for a slab plasma and by Cross (1988a) and Ballico and Cross (1989) for a cylindrical plasma. The effects of finite electron mass have been discussed by Cross and Miljak (1993). For a vacuum boundary, the surface wave satisfies the dispersion relation, $2k_z^2 = k_a^2$. and an eigenmode resonance can be expected for antennas which possess this k_z in their parallel wavenumber spectrum. For $k_z >> k_a$ in the SOL there is little difference between the cut-off fast wave and the SW solutions and for $2k_z^2 = k_a^2$ the SQEW is evanescent everywhere in the plasma. Consequently if mode conversion is possible within the plasma we do not expect the SOL model to make a great deal of difference.

It can also be shown that for $\Lambda >> k_z, k_a$ and regardless of which model is chosen, the ratio of direct SQEW to fast wave amplitude in the plasma is always given by $-i\Lambda/k_S$ where k_S is given by equation (4d). The direct SQEW is therefore not strongly affected by the vacuum boundary in this model.

If a realistic damping is included in these calculations, the SQEW excited or reflected at the ARL undergoes interference with itself after reflection at the plasma vacuum interface and is observed to form high Q resonances (Ross, Chen and Mahajan, 1982; Donnelly and Cramer, 1986; Li, Ross and Mahajan 1989). In the calculations relevant to Fig. 1 however, the SQEW cannot undergo reflection because there is neither a vacuum boundary, metallic antenna nor a conducting wall. Such resonances have never been observed experimentally and it may be that in a real plasma either the damping is higher than expected or the short wavelength SQEW is scattered by limiters and antennas located in the SOL.

In the case of a cylindrical plasma, the geometry acts to increase the amplitude of the SW inside the plasma so that the results of this paper underestimate the antenna coupling efficiency for the mode converted shear wave. A realistic treatment should also include the effects of finite frequency. We may conclude from the present results at modest damping however that the homogeneous plasma model may be used at finite frequency to estimate the power coupled to the directly excited shear wave, whilst a simple finite frequency MHD code for the same antenna can be used to calculate the antenna coupling efficiency to the shear wave excited by FWRMC.

6 DISCUSSION

In this paper, we have established the relationship between the directly excited shear Alfven wave of a homogeneous plasma and that of a one dimensionally inhomogeneous plasma. In particular we now have a plausible theory of direct shear Alfven wave propagation in laboratory plasmas and a primitive comparison between this process and shear Alfven wave excitation by fast wave resonant mode conversion.

Although the profiles shown in Fig. 6 indicate that the directly excited wave and the mode converted wave have a similar structure, it must be borne in mind that for a real antenna, the appearance of the two waves would be quite different. Summation of the wavevector components for the direct SQEW leads to a localised structure which "images" the form of the antenna along the field lines intersecting the antenna. The mode converted wave on the other hand will be influenced by the dispersion of the fast wave. The directly excited SQEW is therefore similar to that of an infinite homogeneous plasma. This also shows that the resonance cone predicted by cold plasma theory with finite electron mass and verified experimentally by Ono (1979) and the guided beams of Borg *et. al.* (1985,1987) are as expected for an inhomogeneous plasma.

Work has only just begun to investigate the applications of slow waves to fusion plasmas. Ono (1993) has reviewed some experimental studies of slow waves and has suggested using the directly excited SQEW (CES ICW) to remove helium ash from the plasma periphery by selective edge heating. Recent experimental results also suggest that Alfven waves may be employed for efficient plasma formation in a stellarator (Lysojvan *et. al.* 1992,1993) where different couplers are required for plasma breakdown and high density formation. These applications rely on a good understanding of the properties of the shear Alfven wave and its excitation mechanisms. The shear Alfven wave may also influence transport given the large RF density perturbation predicted from equation (6). During Alfven wave heating experiments with excited powers in the range of 100 kW and $\omega/\omega_{ci} = 0.2$, large RF edge density perturbations have indeed been observed with amplitudes comparable to the quiescent edge density (Borg *et. al.* 1993).

Acknowledgements

The author would like to acknowledge the support of a QEII fellowship and some ··seful discussions with Prof. R.L. Dewar.

References

ABRAMOWITZ M. and I. A. STEGUN. I. A. (1970a) *'Handbook of Mathematical Functions'.* Dover Publications p. 447, 10.4.32.

ABRAMOWITZ M. and I. A. STEGUN. I. A. (1970b)*' Handbook of Mathematical Functions'.* Dover Publications p. 376, 9.6.21.

BALLICO M.J. and CROSS R.C. (1989) Plasma Phys. and Contr. Fusion 31, p. 1141

BELLAN P. M. and PORKOLAB M. (1974) Phys. Fluids 17, 1592.

BLEISTEIN N. and HANDELSMANN. A. (1975a) *'Asymptotic Expansions of Integrals '* Dover Publications. p. 265.

BLEISTEIN N. and HANDELSMANN. A. (1975b) *'Asymptotic Expansions of Integrals '* Dover Publications p. 50.

BORG G. G. (1987) PhD Thesis, The University of Sydney.

BORG G.G. and CROSS R.C. (1987) Plasma Phys. and Contr. Fusion 29, 681.

BORG G.G., BRENNAN M. H., CROSS R. C., GIANNONE L. and DONNELLY I.J. (1985) Plasma Phys. Contr. fusion 27, 1125.

BORG G.G., LISTER J.B. DALLA PIAZZA S and MARTIN Y (1993) Nuc. Fusion 33, 841.

CHEN L. and HASEGAWA A. (1974) Phys. Fluids 17, 1399.

CROSS R.C. (1988a) *'An Introduction to Alfven Waves'* Adam Hilger.

CROSS R.C. (1988b) Plasma Phys. and Contr. Fusion 30, 1213.

CROSS R.C. and LEHANE J. A. (1968) Phys. Fluids 11, 2621.

CROSS R.C. (1983) Plasma Physics 25, 1377.

CROSS R.C. and MILJAK D. (1993) Plasma Phys. and Contr. Fus. 35, 235.

B. DAVIES (1978) *'Integral Transforms and their Applications'.* Springer-Verlag New York. pp. 359 - 365.

DONNELLY I. J. and CRAMER N. F. (1986) J. Plasma Physics 35, 75.

FAULCONER D. W. (1980) Physics Letters 75A, 355.

FEJER J.A. and LEE K.F. (1967) J. Plasma Physics 1, 387.

HASEGAWA A. and UBEROI C. (1982) *'The Alfven Wave'* Tech. Inf. Centre, U.S. D.O.E.

HASEGAWA A. and CHEN L. (1974) Phys. Rev. Letts. 32, 454

HASEGAWA A. and CHEN L. (1976) Phys. Fluids 19 1924.

HASEGAWA A. and CHEN L. (1975) Phys. Rev. Letts. 35, 370.

Li W-Q, Ross D.W and Mahajan S.M. (1989) Phys. Fluids B. 1 2353.

LYSOJVAN A.I., MOISEENKO V. E., SHVETS O. M. and STEPANOV K.N. (1992) Nuc. Fusion 32, 1361.

LYSOJVAN A.I., MOISEENKO V.E., PLYUSNIN V.V., KASILOV S.V., BONDARENKO V.N., CHECHKIN S.V., FOMIN I.P., GRIGOR'EVA L.I., KANOVALOV V.G., KOVAL'OV S.V., LITVINOV A.P., MIRONOV Y.K., NAZAROV N.I., PAVLICHENKO O.S., PAVLICHENKO R.O., SHAPOVAL A.N., SHIBENKO A.I. and VOLKOV E.D. (1993) *"The Study of Three-Half-Turn and Frame-type Antennas ffor ICRF Plasma Heating in the Uragan 3-M Torsatron" 5th International Toki Conference, 16th - 19th Nov.* (1993). (Submitted to Fusion Engineering and Design)

MURPHY A.B. (1989) Plasma Phys. and Contr. Fusion 31, 21.

NGAN Y. C. and SWANSON D.G. (1977) Phys. Fluids 20, 1920.

PURI S. (1987a) Nuc. Fusion 27, 229 .

PURI S. (1987b) Nuc. Fusion 27, 1091.

ONO M. (1993) *'Investigation of electrostatic waves in the ion cyclotron range of frequencies in L-4 and ACT-1'* Report PPPL-2900 Princeton.

ONO M. (1979) Phys. Rev Letts. 42, 1267

PERKINS F. W. (1977) Nuc. Fusion 17, 1197.

ROSS D.W., CHEN G. L. and. MAHAJAN S.M (1982) Phys. Fluids 25, 652.

ROSS D.W., Li YANMING,. MAHAJAN S.M. and MICHIE R.B. (1986) Nuc. Fusion 26, 139.

SHOUCRI M., MORALES G.J. and MAGGS J.E. (1985) Phys. Fliuds 28, 2458.

STIX T. H., (1980) Proc. 2nd Varenna-Grenoble Symp. on Plasma Heating in Toroidal Plasmas 2, p. 631.

STIX T.H. (1992a) *'Waves in Plasmas'* American Institue of Physics, New York. pp. 373 - 379

STIX T.H. (1992b) *'Waves in Plasmas'* American Institue of Physics, New York. pp. 70 - 77.

STIX T. H. (1965) Phys. Rev. Letters 15, 878.

SWANSON D.G. (1989) *'Plasma Waves'* Academic Press Inc.

SY W.N.-C (1984) Plasma Phys. and Contr. Fusion 26, 915.

VACLAVIK J. and APPERT K. (1991) Nuc. Fusion 31, 1945.

WEISEN H., APPERT K., BORG G.G., JOYE B., KNIGHT A.J. LISTER J.B. and VACLAVIK J. Phys. Rev. Letts. (1989) 63, 2476.

FIGURE CAPTIONS

Figure 1. Slab geometries for a) the infinite homogeneous plasma and b) the linear density gradient with a uniform plasma scrape-off layer.

Figure. 2 Contours in the complex u-plane for,
a) the representation of the McDonald function in equation (22).
b) the solution of equations (23) and (25) for $X > 0$.
c) the solution of equations (23) and (25) for $X < 0$.
The saddle-points are marked with crosses and the shaded regions represent the valleys along which the inversion integral has to be performed.

Figure 3. The level curves of the real part of V(u) in equation (23). The symbols V and H refer to valleys and hills respectively. The saddle points occur where V(u) has a stationary point, $V'(u) = 0$. These are marked with crosses.
a) For $X > 0$
b) For $X < 0$

Figure 4. Contours in the complex p-plane for,
a) the representation of the Ai-Airy function in equation (29).
b) the solution of equations (17) for $X > 0$ using the contours $C_1 \cup C_2$ and $X < 0$ using the contour C_3.

Figure 5. The level curves of the real part of w(p) in equation (18). The symbols V and H refer to valleys and hills respectively. The saddle points occur where V(u) has a stationary point, $V'(u) = 0$. These are marked with crosses.
a) For $X > 0$
b) For $X < 0$

Figure 6. A representative plot of the E_y wavefield excited by the antenna with $k_a = 1.0$, $k_z = 2.0$, $k_y = 20$ radians per metre, $\Delta = 0.05$ m and modest damping where $\gamma = (1 + 0.05i) \times 10^{-3}$. The geometry is that of Fig. 1b, the antenna is located at $x = -b = -.027$ m and the Alfven resonance layer at $x = .15$ m.

Figure 7. The unbroken curve is the ratio of the power coupled to the directly excited SQEW (P_D) to that of the SQEW excited by FWRMC (P_M) as calculated from equation (36) for $\gamma = (1 + 0.05i) \times 10^{-3}$. The points are the computed ratio of the power coupled by the antenna to the SQEW to that coupled to the fast wave for the same value of $\gamma = (1 + 0.05i) \times 10^{-3}$.

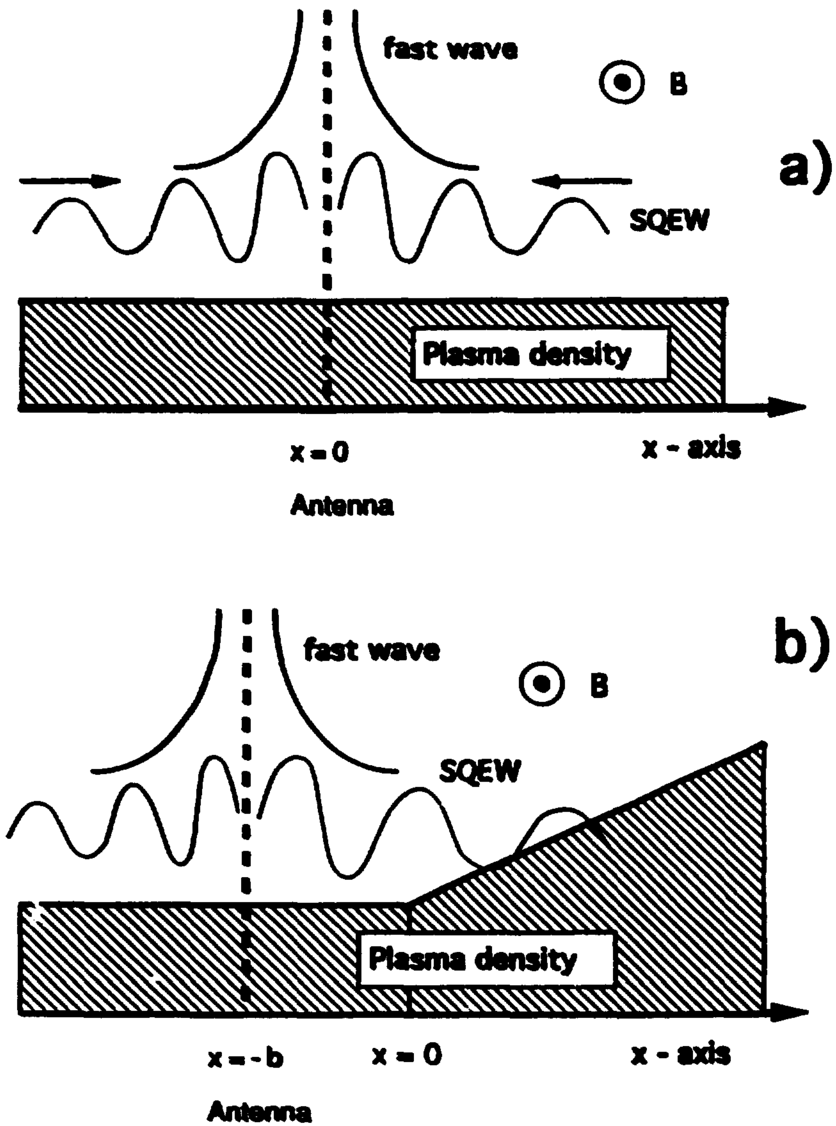
fast wave
B
a)
SQEW
Plasma density
x = 0
x - axis
Antenna
fast wave
B
b)
SQEW
Plasma density
x = - b
x = 0
x - axis
Antenna

Fig 1

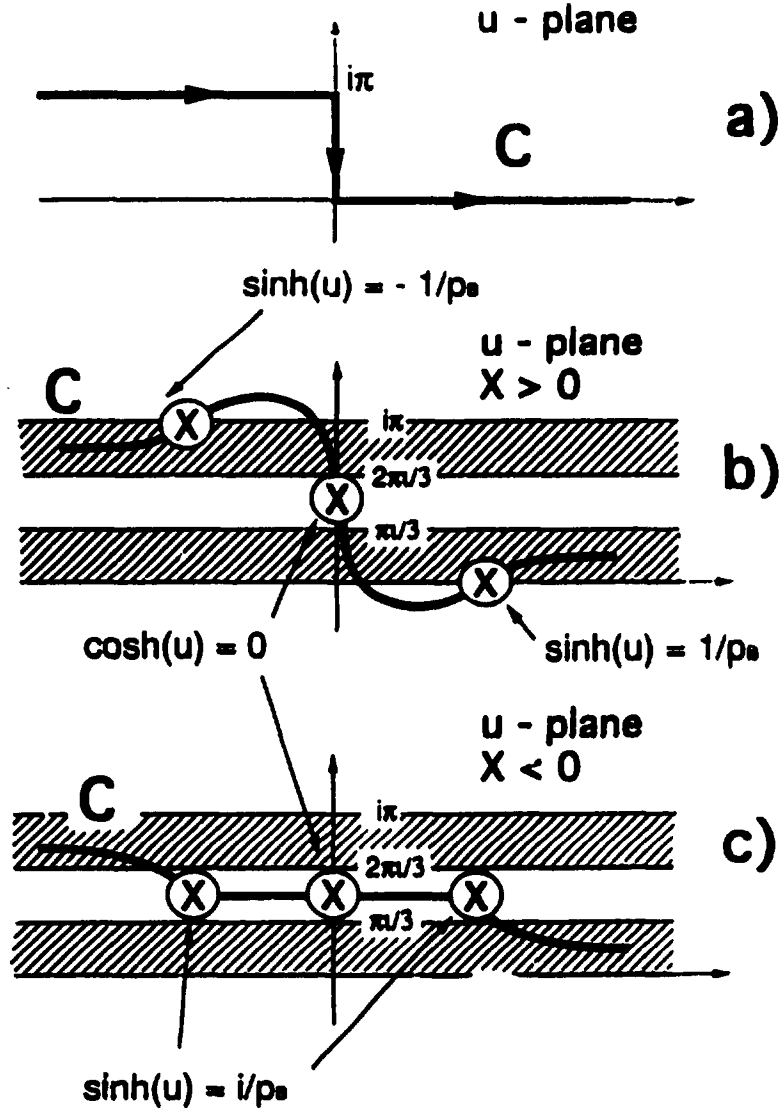
u - plane
iπ
a)
C
sinh(u) = - 1/pₑ
u - plane
X > 0
C
iπ
2π/3
b)
π/3
cosh(u) = 0
sinh(u) = 1/pₑ
u - plane
X < 0
C
iπ
2π/3
c)
π/3
sinh(u) = i/pₑ

Fig 2

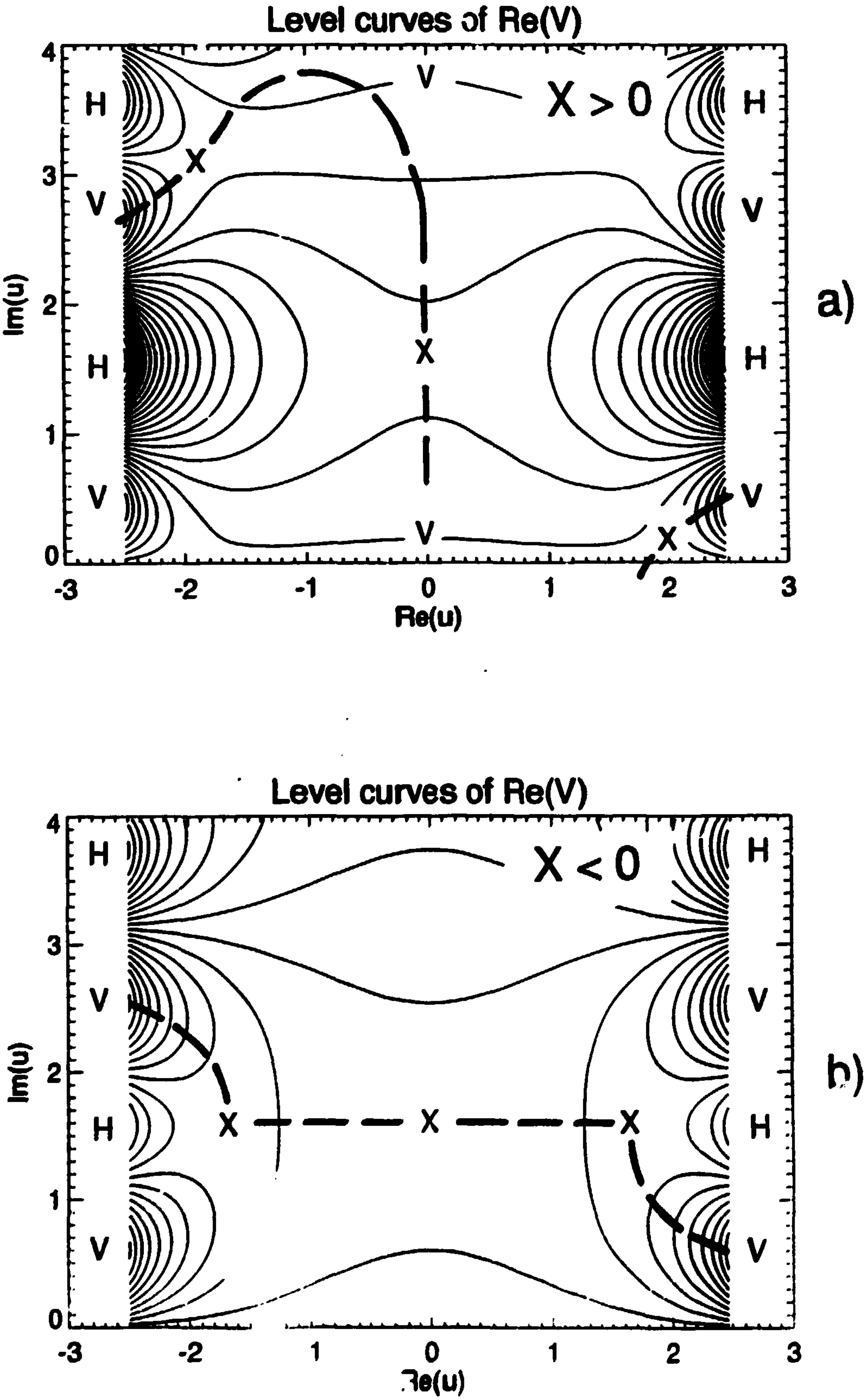

Fig 3

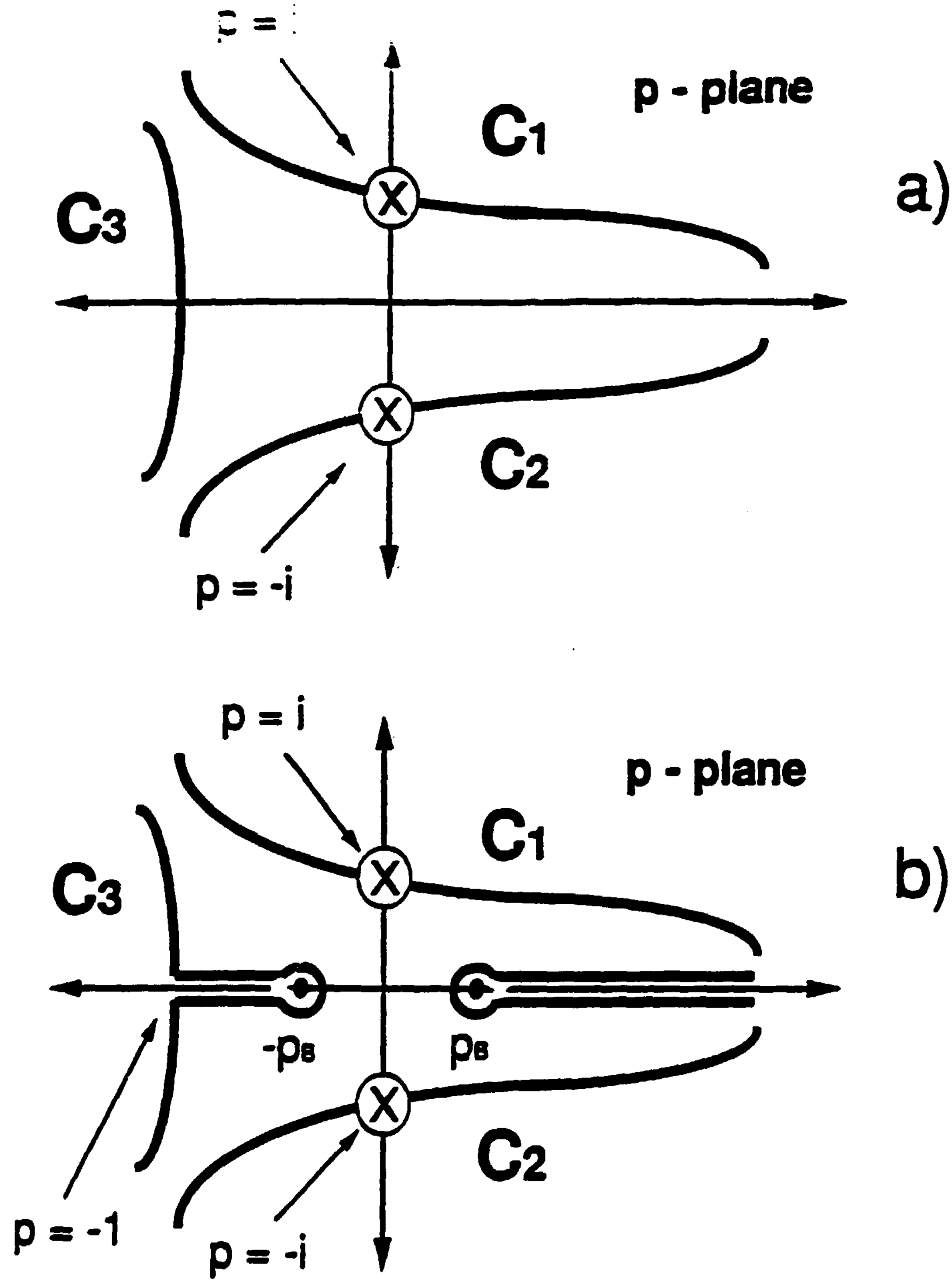

Fig 4

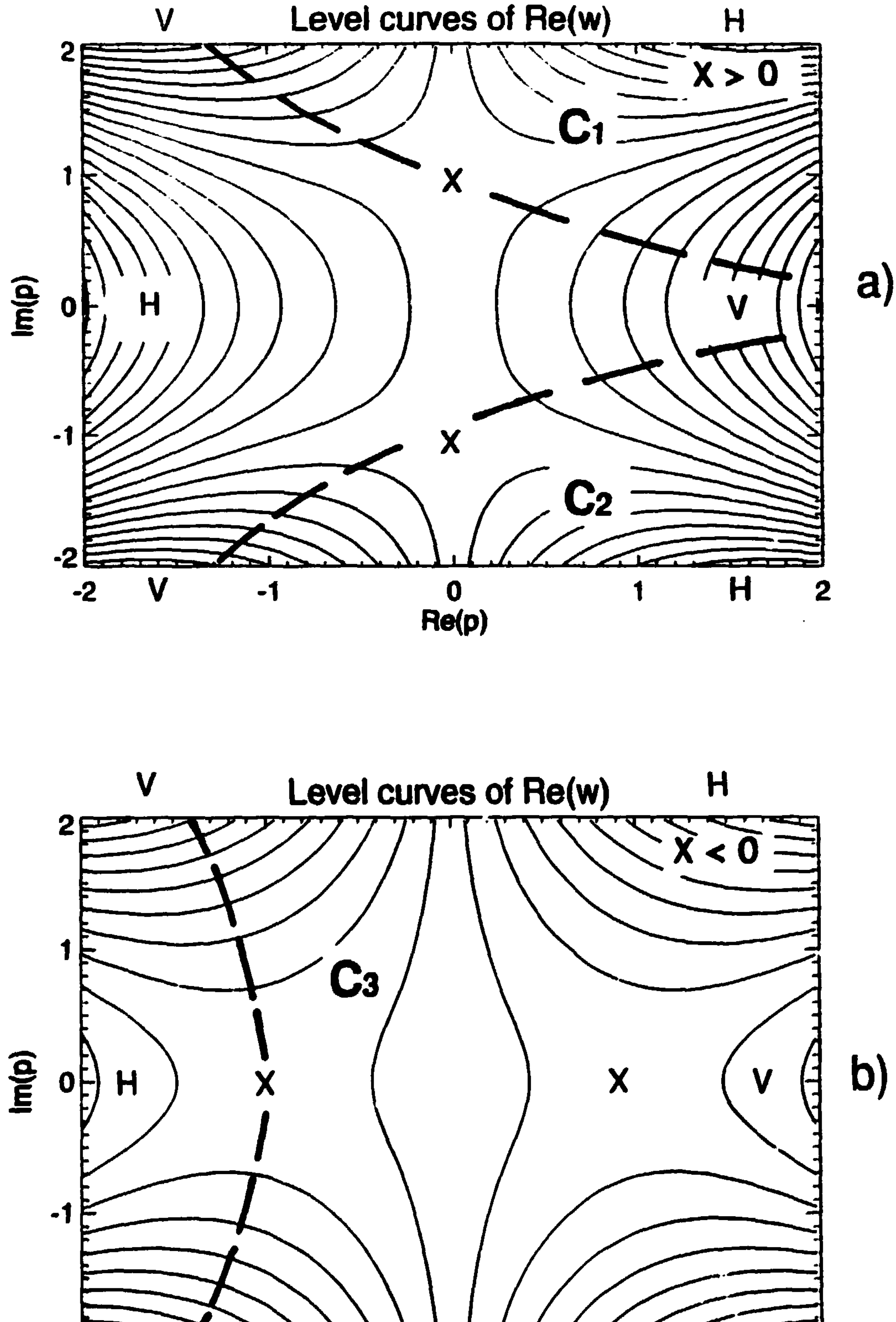
Level curves of Re(w)
X > 0
C1
C2
Im(p)
Re(p)
V
H
X
a)
Level curves of Re(w)
X < 0
C3
Im(p)
Re(p)
V
H
X
b)

Fig 5

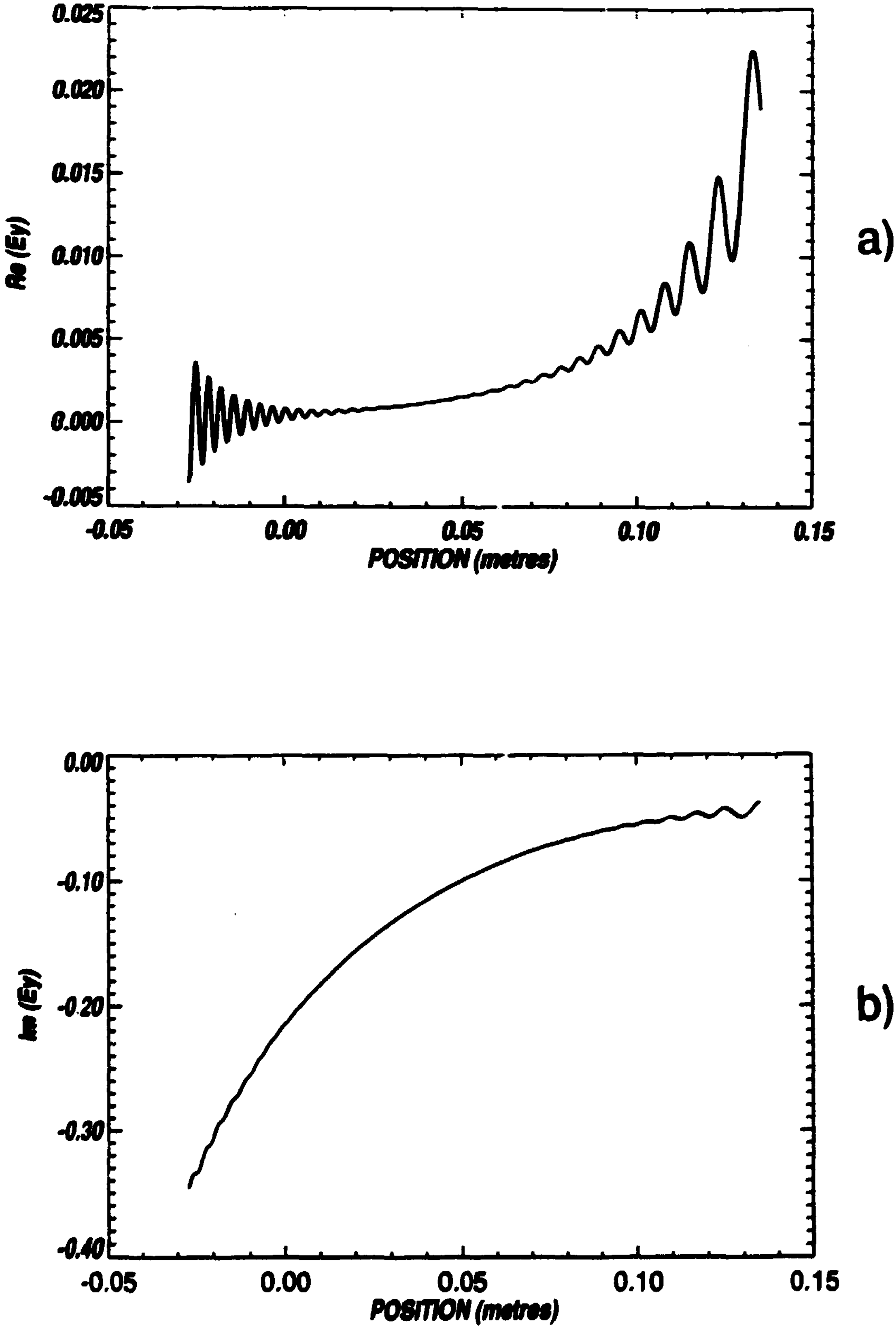
a)
Re (Ey)
0.025
0.020
0.015
0.010
0.005
0.000
-0.005
-0.05
0.00
0.05
0.10
0.15
POSITION (metres)
b)
Im (Ey)
0.00
-0.10
-0.20
-0.30
-0.40
-0.05
0.00
0.05
0.10
0.15
POSITION (metres)

Fig 6.

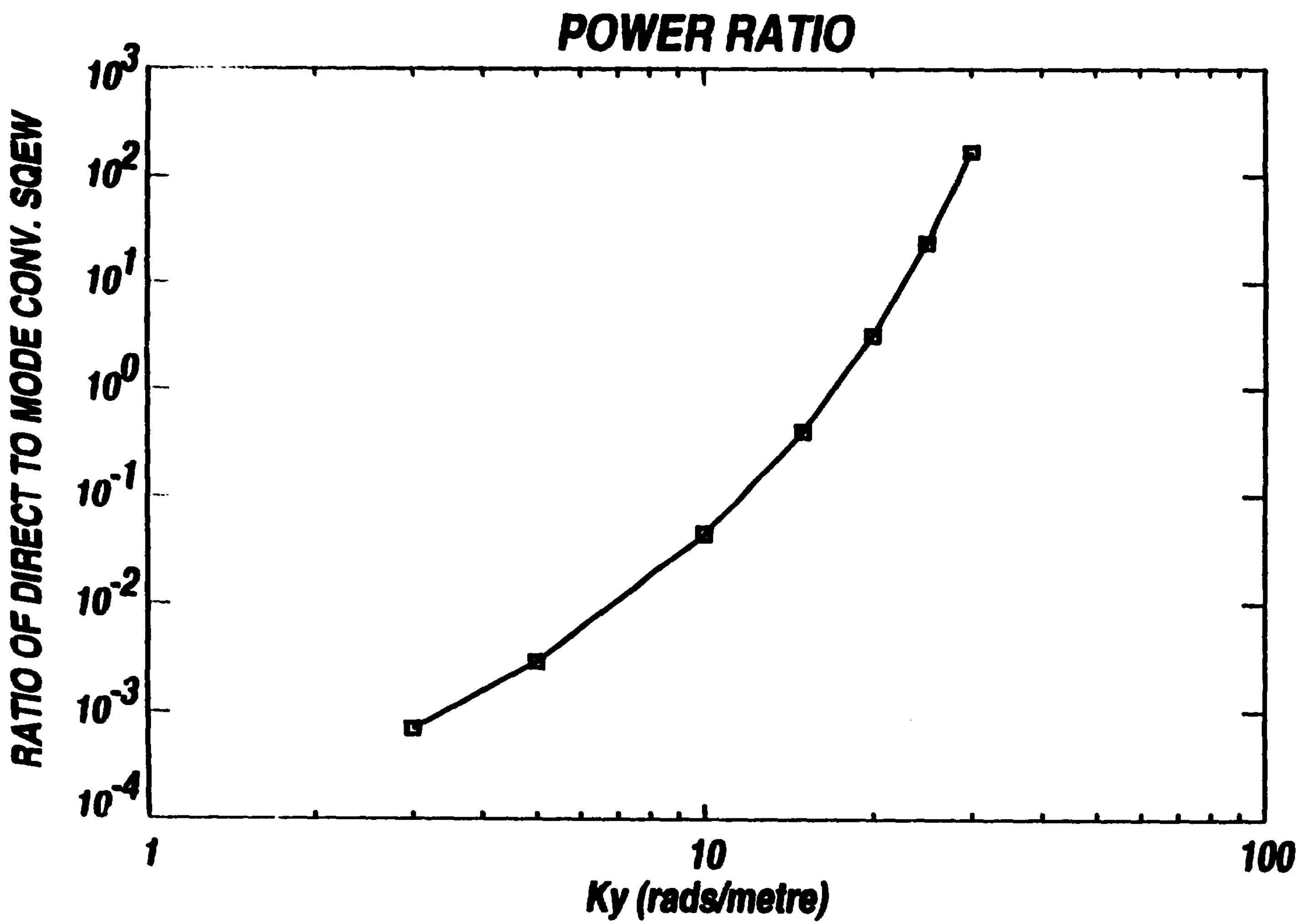
POWER RATIO
RATIO OF DIRECT TO MODE CONV. SQEW
10^{3}
10^{2}
10^{1}
10^{0}
10^{-1}
10^{-2}
10^{-3}
10^{-4}
1
10
100
Ky (rads/metre)

Fig 7